Dedicated to Academician Aureliu Sandulescu's 80^{th} Anniversary

METALLIC ATOMIC CLUSTERS

D. N. POENARU[1,a,2], R. A. GHERGHESCU[1,2], W. GREINER[2]

[1]Horia Hulubei National Institute for Physics and Nuclear Engineering,
Reactorului 30, RO-077125 Măgurele-Bucharest, Romania
Email: [a]poenaru@nipne.ro
[2]Frankfurt Institute for Advanced Studies,
Ruth-Moufang-Str. 1, D-60438 Frankfurt am Main, Germany

Received October 6, 2011

The nuclear liquid drop model and the the shell correction method, have been adapted for neutral and charged atomic clusters. We used the macroscopic-microscopic method to investigate neutral hemispheroidal atomic clusters deposited on a surface.The electrostatic energy of charged metallic clusters is studied for hemispheroidal and cylindrical shapes. The maximum value of Coulomb energy of a Na_{54}^{2+} cluster takes place at a superdeformed prolate shape. A finite value of the electric charge makes the cluster less stable and decreases the value of equilibrium deformation. The most important yield in fission of charged metallic clusters is usually obtained when the light fragment is a singly charged trimer, the analog of an α-particle with magic number of delocalized electrons $n_e = 2$. In this case both the shell corrections and the LDM deformation energy have minima at the same mass asymmetry which corresponds to the trimer emission.

Key words: Liquid drop model, Coulomb energy, surface energy, charged metallic atomic clusters, stability of clusters, alkali metals, shell effects.

PACS: 36.40.Wa, 36.40.Qv, 71.45.-d, 71.20.Dg.

1. INTRODUCTION

The density functional theory [1] is successfully employed in the field of atomic cluster physics. Alternatively, with less computational effort, one can use some simple models [2] replacing the many-body effects by an effective single-particle potential, since to a good approximation the delocalized conduction electrons of neutral small metallic clusters form a Fermi liquid like the atomic nucleus [3]. The liquid drop model (LDM) [4] and the shell correction method [5, 6], were used to study neutral and charged atomic clusters.

By analyzing some shapes of cluster deposited on a surface obtained by using scanning probe microscopy [7, 8], one can see that a hemispheroid with the z axis of cylindrical symmetry oriented perpendicularly on the surface plane may be a good approximation. Since 2007 we adapted the macroscopic-microscopic method to hemispheroidal atomic clusters deposited on a planar surface [9–14]. The interdisciplinary character of our research work was particularly stressed in several pub-

lications [15–18] including those on trimer emission from charged metallic clusters.

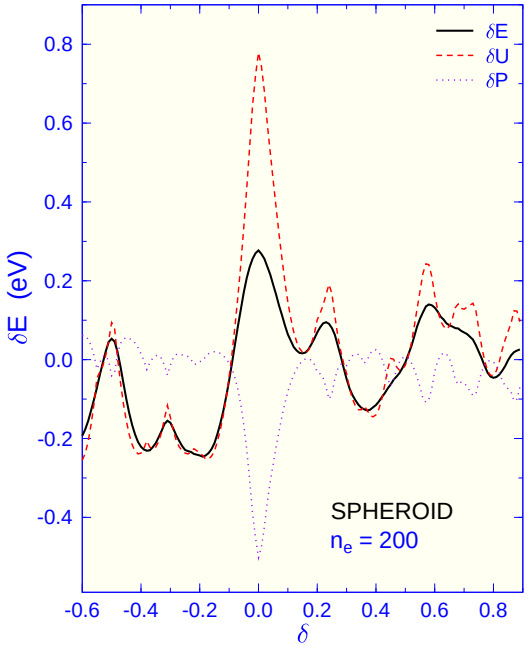

Fig. 1 – Shell and pairing corrections vs. deformation δ for a spheroidal Na_{210}^{10+} cluster.

According to the macroscopic-microscopic method (MMM), the deformation energy is given by

$$E = E_{LD} + \delta E = E_{LD} + \delta U + \delta P \tag{1}$$

in which E_{LD} is the liquid-drop term, δU is the shell correction, δP is the pairing correction and $\delta E = \delta U + \delta P$. An example is given in figure 1 for a spheroidal Na_{210}^{10+} cluster. The amplitudes of shell and pairing corrections are as low as few fractions of an eV. Spherical magic numbers: 2, 8, 40, 58, 92,136, 198, 264, 344, 442, 554, 680, 800, 970, 1120, 1310, 1500, ...

We used LDM and the MMM to investigate neutral spheroidal and hemispheroidal atomic clusters deposited on a planar surface. Analytical relationships for the deformation-dependent LDM energies of prolate [9] and oblate [13, 19] hemispheroidal atomic clusters have been obtained. A superdeformed prolate hemispheroid was found to be the most stable shape within LDM. It is also the shape with maximum degeneracy of quantum states of the hemispheroidal harmonic oscillator based single-particle model [10, 12, 20]. This new shell model (quantum harmonic hemispheroidal oscillator) posses striking properties of symmetry, which exhibits the

maximum degeneracy at a super-deformed prolate shape (ratio of semiaxes 1/2). Another single-particle shell model [21] is devoted to prolate short-cup shapes [22]. The shell and pairing corrections added to the LDM deformation energy allow to calculate potential energy surfaces (PES) [11, 23–25] and to determine equilibrium shapes in the ground-state or shape isomeric states.

Charged metallic clusters [26] are particularly interesting to study from the stability point of view, having in mind their decay by fission. When we compare the LDM PES with the shell and pairing corrections, δE, for nuclei we always have the minimum energy E_{LDM} at a zero mass asymmetry, $\eta = 0$, but the minima of δE are usually positioned at different mass asymmetry determined by the occurrence of magic numbers of nucleons. It was experimentally proven that the most important yield in fission of charged metallic atomic clusters is usually obtained when the light fragment is a singly charged trimer (the analog of an alpha-particle with magic number of delocalized electrons $n_e = 2$). Our calculations for charged alkali clusters are showing that both the E_{LDM} and δE energies are possessing local minima at the same mass asymmetry corresponding to this "alpha-cluster" [15].

In the present work we present the results concerning the influence of the electric charge on the stability of two kinds of shapes: hemispheroids and cylinders, as well as on fission of charged metallic clusters.

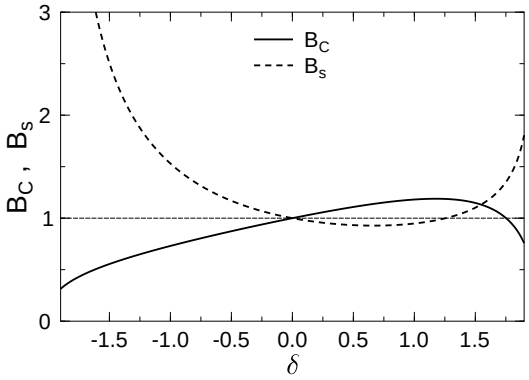

Fig. 2 – The relative deformation energies B_C and B_s of a hemispheroidal Na_{54}^{2+} cluster.

2. HEMISPHEROIDAL SHAPES

The spheroidal deformation δ ($delta < 0$ oblate, $delta > 0$ prolate) is defined as a function of dimensionless semiaxes a, c (units of $R_0 = r_s N^{1/3}$ for spheroid and

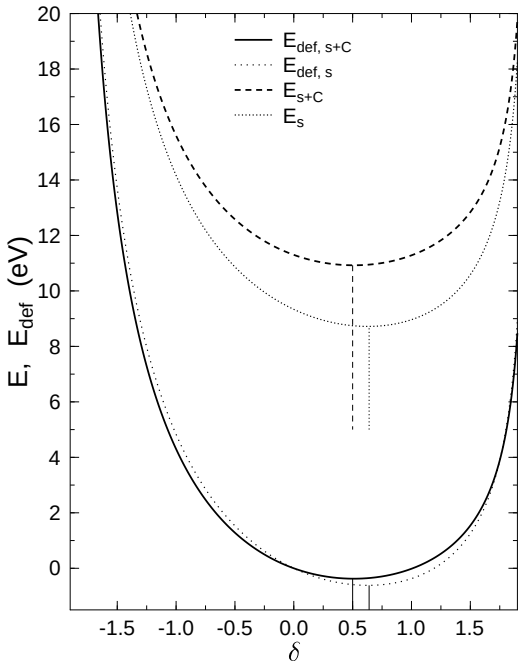

Fig. 3 – LDM surface and Coulomb energies of a hemisperoidal Na_{54}^{2+} cluster. $E_{def,s}$ and $E_{def,s+C}$ are the deformation energies relative to zero deformation energy. The volume energy, which is not dependent on deformation was not taken into account.

of $R_s = 2^{1/3}R_0$ for hemispheroid)

$$a = \left(\frac{2-\delta}{2+\delta}\right)^{1/3} \; ; \; c = \left(\frac{2+\delta}{2-\delta}\right)^{2/3} \tag{2}$$

In figure 2 we plotted the relative Coulomb and surface energies versus deformation of a doubly charged hemispheroidal Na cluster with 54 atoms (52 delocalized electrons). Their absolute values are shown in figure 3.

The maximum value of Coulomb energy is reached at a superdeformed prolate shape. It is clear that a finite value of the Coulomb energy makes the cluster less stable (the minimum of the absolute value of energy is increased). The minimum of energy (equilibrium deformation) is moved to smaller deformation, $\delta = 0.50$ instead of $\delta = 0.64$.

We can also add the shell and pairing corrections. The influence of the electric charge on the equilibrium deformation of a hemispheroidal shape is illustrated in figure 4 on the example of Na_{190} cluster starting from being neutral (at the bottom of the figure), then ionized z times, where $z = 2, 4, 6, 8, 10$. The variation of shell corrections with deformation parameter (on the left hand side) corresponding

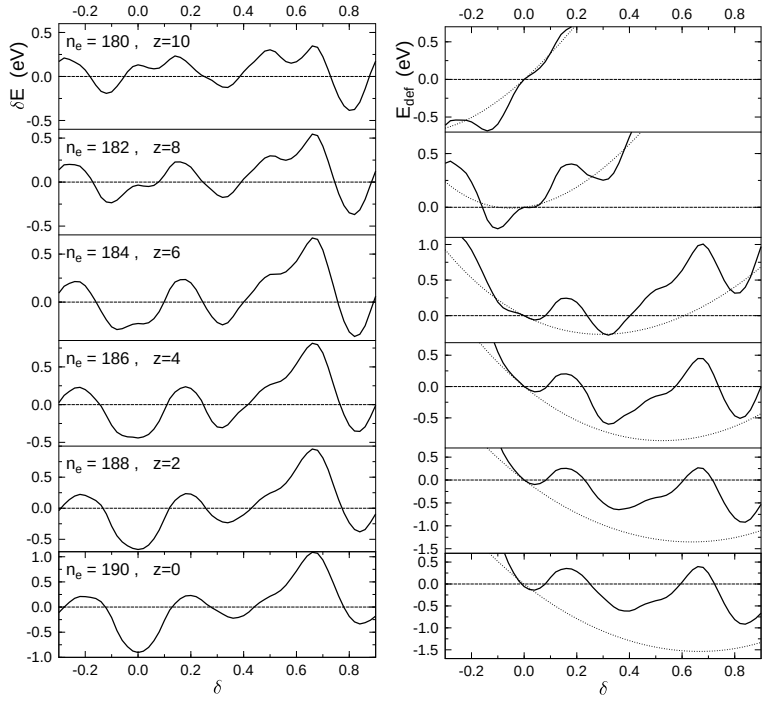

Fig. 4 – Variation of the shell corrections, δE, (left hand side) and of the LDM energy (dotted line), E_{LDM}, and the total deformation energy (solid line) $E_{def} = E_{LDM} + \delta E$ (right hand side) versus the deformation, δ, for a hemispheroidal Na cluster with 190 atoms and different charges $z = 0, 2, 4, 6, 8, 10$.

to different values of z are different because the number of delocalized electrons are $n_e = 190 - z$. The LDM and total equilibrium deformation decreases when z increases. For applications in which the substrate should be entirely covered with deposited cluster, the efficiency increases when the clusters are charged: with 60% when the equilibrium deformation δ_{eq} decreases from 0.66 to 0.

3. CYLINDRICAL CLUSTER

The body taken as a reference corresponds to a radius $a_0 = 1$ and a height $c_0 = 2$, for which the volume $V_0 = 4\pi R_0^3/3 = \pi R_{c0}^3 a_0^2 c_0 = 2\pi R_{c0}^3$, where $R_{c0} = (2/3)^{1/3} R_0$ and the volume conservation leads to $a^2 c = 2$.

The deformation parameter is defined a $\xi = c/a$ so that $\xi_0 = 2$. The surface area

$$S = 2\pi R_{c0}^2 a^2 + 2\pi R_{c0}^2 ac = 2\pi R_{c0}^2 a(a + c) \tag{3}$$

so that

$$E_{sc} = S\sigma = a(c+a)E_{sc}^0/3 \tag{4}$$

The Coulomb energy double integral is computed numerically. From numerical quadrature we obtain $E_{Coul-c}^0 = 0.494095855522E_C^0$ i. e. the cylinder with $h = 2a$ has an energy smaller than the sphere by about 51 %.

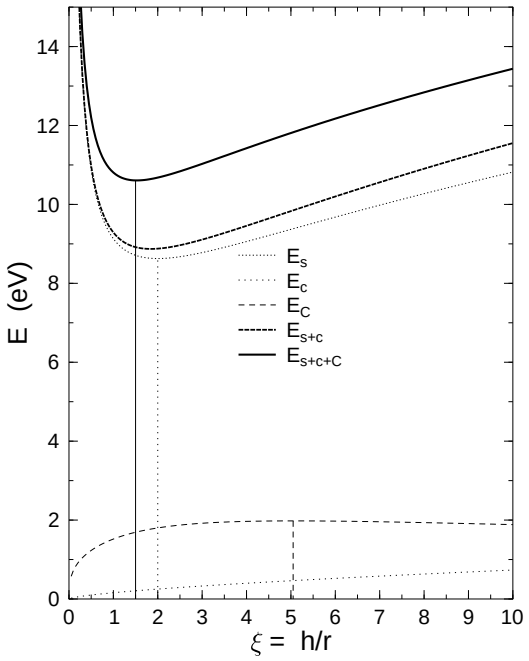

Fig. 5 – LDM energies of a cylindrical cluster Na_{54}^{2+}.

In figure 5 we plotted the surface, curvature, and Coulomb energies versus the deformation ξ of a doubly charged cylindrical Na cluster with 54 atoms and 52 delocalized electrons. We calculate this time the curvature energy just to show how small it is compared to the surface energy.

With Coulomb energy (max. at $\xi = 5.05$) the minimum moved to smaller deformation $\xi = 1.50$ instead of $\xi = 2.00$. Also the stability decreases: the minimum of the absolute value of energy is increased.

4. FISSION OF A CHARGED METALLIC CLUSTER

A neutral cluster with N atoms of a metal with valence $v = 1$ will have $n_e = N$ delocalized electrons. The number of delocalized electrons left after ionization or electron attachment are $n_e = N - z$ for a cation and $n_e = N + z$ for an anion, where

z is called the excess charge and N the size of the cluster. In the most frequently studied fission ("Coulomb explosion") process

$$\mathbf{M_N^{z+}} \rightarrow \mathbf{M_{N_1}^{z_1+}} + \mathbf{M_{N_2}^{z_2+}} \tag{5}$$

we have $n_e = n_{e1} + n_{e2}$ and $z = z_1 + z_2$. The parent is doubly charged ($z = +2$) so that the fragments are single ionized: $z_1 = z_2 = 1$. The numbers of electrons are conserved: $N = N_1 + N_2$; $z = z_1 + z_2$; $n_e = N - z = n_{e1} + n_{e2}$; $n_{ei} = N_i - z_i$. Charged clusters are produced by photoionization with laser beams, or by collision. The ionization energy of metals is generally much lower than the ionization energy of nonmetals hence metals will generally lose electrons to form cations while nonmetals will generally gain electrons to form anions. The fission channel with the trimer fragment M_3^{+1}, having a magic number of delocalized electrons $n_e = 2$, is very frequently the predominant one, in analogy to α-decay of nuclei (see *e.g.* fission of K^{2+} NaK^{2+} [27]; of Li^{2+} and K^{2+} [28]; of $Na^{2+\ to\ 7+}$, $K^{2+\ to\ 7+}$, $Rb^{2+\ to\ 7+}$, and $Cs^{2+\ to\ 7+}$ [29], and of Ag^{2+} [30]). Deformation energy

$$E_{LDM} = E - E^0 = (E_s - E_s^0) + (E_C - E_C^0) = E_s^0(B_s - 1) + E_C^0(B_C - 1) \tag{6}$$

For spherical shapes: $E_s^0 = 4\pi R_0^2\sigma = a_s n_e^{2/3} = 4\pi r_s^2 n_e^{2/3}$; $E_{C-metal}^0 = z^2e^2/(2R_0) = z^2e^2/(2r_s n_e^{1/3})$ for a surface distribution of charge. A charged cluster is stable as long as its fissility is smaller than one

$$Fissility\ \ X = \frac{E_c^0}{2E_s^0} = \frac{e^2}{16\pi r_s^3\sigma}\frac{z^2}{n_e} < 1\ ; \quad n_e > n_c = \frac{e^2z^2}{16\pi r_s^2\sigma} \tag{7}$$

Very light charged clusters are unstable. One should take into account the special

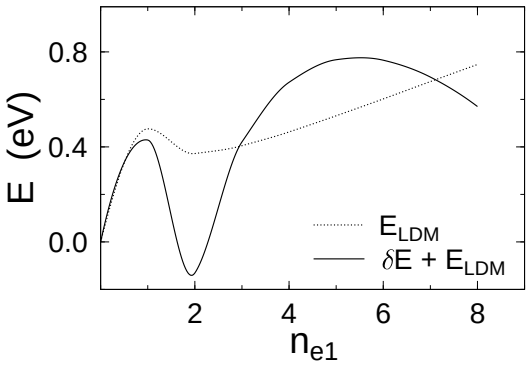

Fig. 6 – Details of the large asymmetry part of scission point deformation energies E_{LDM} (dotted line) and $E_{LDM} + \delta E$ (full line) for fission of a Cs cluster with 64 atoms and a charge $z = 4$.

behavior of a charged metallic cluster when the Coulomb energy is calculated: unlike the bulk distribution of the charge in nuclei, here we have a surface density σ_e [31,

32]. The electrostatic energy of a charge distribution

$$E_C[\sigma_e] = \frac{1}{2}\int\int \frac{\sigma_e(\mathbf{r})\sigma_e(\mathbf{r}_1)d^2\mathbf{S}d^2\mathbf{S_1}}{|\mathbf{r}-\mathbf{r}_1|} \tag{8}$$

The distribution σ_e on the surface is obtained by minimizing the energy under the constraint $Q = ze = \int \sigma_e(\mathbf{r})d^2\mathbf{S}$ *i.e.* the functional derivative

$$\frac{\delta(E-\lambda Q)}{\delta\sigma_e} = \frac{1}{2}\int \frac{\sigma_e(\mathbf{r}_1)d^2\mathbf{S_1}}{|\mathbf{r}-\mathbf{r}_1|} - \lambda = 0 \tag{9}$$

The polarizabilities of the two fragments has to be taken into account when we calculate the Coulomb interaction. One can use the image charge method [33] or the simpler approach [30]. From the figure 6 one can see that both LDM and shell correction energies are favoring the singly charged trimer emission at $n_{e1} = 2$.

5. RELEASED ENERGY

Within the liquid drop model (LDM) for charged metallic clusters the dissociation energy (Q-value) for this reaction, assuming spherical shapes [27] may be written as a sum of surface, Coulomb and ionization contributions

$$Q = Q_s + Q_C + Q_{IP} \tag{10}$$

$$Q_s = a_s[n^{2/3} - p^{2/3} - (n-p)^{2/3}] \tag{11}$$

$$Q_C = \frac{e^2}{2r_s}\left[\frac{z^2}{n^{1/3}} - \frac{z_1^2}{p^{1/3}} - \frac{(z-z_1)^2}{(n-p)^{1/3}}\right] \tag{12}$$

$$Q_{IP} = \frac{e^2}{8r_s}\left[\frac{z_1}{p^{1/3}} + \frac{(z-z_1)^2}{(n-p)^{1/3}} - \frac{z}{n^{1/3}}\right] \tag{13}$$

where $n = n_e,\ p = n_{e1},\ n-p = n_{e2}$, $a_s = 4\pi r_s^2\sigma$ is the surface energy constant proportional to the surface tension σ, $e^2/2 = 7.1998259$ eV·Å. Experimental results are showing minima of the LDM fission barrier $E_{12} - Q$ for $p = 2$, like in figure 6. As suggested by the figure 7, this may be simply explained within LDM by plotting the derivative dQ/dp vs. p. It vanishes at a value of p very close to $p = 2$. Due to the smooth variation with p of the interaction energy E_{12} between the separated fragments, the barrier is minimum when the Q-value is maximum.

$$\frac{dQ}{dp} = \frac{dQ_s}{dp} + \frac{dQ_C}{dp} + \frac{dQ_{IP}}{dp} \tag{14}$$

$$\frac{dQ_s}{dp} = \frac{2a_s}{3}\left[\frac{1}{(n-p)^{1/3}} - \frac{1}{p^{1/3}}\right] \tag{15}$$

$$\frac{dQ_C}{dp} = \frac{e^2}{6r_s}\left[\frac{z_1^2}{p^{4/3}} - \frac{(z-z_1)^2}{(n-p)^{4/3}}\right] \tag{16}$$

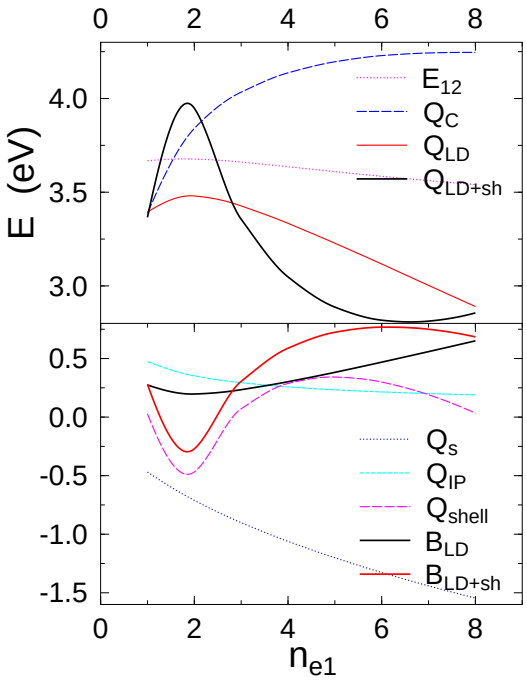

Fig. 7 – Fission of Cs_{100}^{6+} with singly charged light fragments. Q-values and fission barriers. Minimum barrier height and maximum Q-value reached at a very large mass asymmetry corresponding to $p = n_{e1} = 2$.

$$\frac{dQ_{IP}}{dp} = \frac{e^2}{24r_s}\left[\frac{z-z_1}{(n-p)^{4/3}} - \frac{z_1}{p^{4/3}}\right] \tag{17}$$

Unlike in nuclear fission, the low n_{e1} channels (in particular the trimer Na_3^+ fragment) are promoted not only by the shell effects but also by the LDM!

According to LDM (collective properties of fermions) in fusion and fission (including cluster radioactivity and α-decay) of nuclei one should only have mass symmetrical processes $\eta = 0$. The experiments are explained only by adding the quantum shell effects (individual properties of nucleons). *Charged clusters are ideally "alpha" emitters!* By increasing the charge and the ratio a_s/r_s one may obtain large Q-values. They may be used in applications. Deformations and shell effects are usually increasing the Q-values.

Acknowledgments. This work is partially supported by Deutsche Forschungsgemeinschaft, Bonn, partially within IDEI Programme under contract with UEFISCSU, Bucharest, and partially within ANCS Nucleu Programme through project PN-09370102.

REFERENCES

1. R. G. Parr, W. Yang, *Density-Functional Theory of Atoms and Molecules* (Oxford University Press, New York, 1989).
2. W. A. de Heer, in *Metal Clusters at Surfaces*, K.-H. Meiwes-Broyer, ed., pp. 1–35 (Springer, Berlin, 2000).
3. R. Schmidt, R. L. Jaffe, R. M. Dreizler, J. Ehlers, K. Hepp (eds.), *Nuclear Physics Concepts in the Study of Atomic Cluster Physics*, vol. 404 (Lecture Notes in Physics, Springer, Berlin, 1992).
4. L. J. W. S. Rayleigh, Phil. Mag. **14**, 184–186 (1882).
5. V. M. Strutinsky, Nucl. Phys. A **95**, 420 (1967).
6. C. Yannouleas, U. Landman, R. N. Barnett, in *Chapter 4 in Metal Clusters*, W. Ekardt, ed., pp. 145–180 (Wiley, New York, 1999).
7. K. Seeger, R. E. Palmer, Appl. Phys. Lett. **74**, 1627–1629 (1999).
8. B. Bonanni, S. Cannistraro, J. Nanotechnology Online **1**, 1–14, doi: 10.2240/azojono0105 (November 2005).
9. D. N. Poenaru, R. A. Gherghescu, A. V. Solov'yov, W. Greiner, Europhys. Lett. **79**, 63001 (2007).
10. D. N. Poenaru, R. A. Gherghescu, A. V. Solov'yov, W. Greiner, Phys. Lett. A **372**, 5448–5451 (2008).
11. D. N. Poenaru, R. A. Gherghescu, I. H. Plonski, A. V. Solov'yov, W. Greiner, Europ. Phys. J. D **47**, 379–393 (2008).
12. R. A. Gherghescu, D. N. Poenaru, A. V. Solov'yov, W. Greiner, Int. J. Mod. Phys. B **22**(28), 4917–4935 (2008).
13. D. N. Poenaru, R. A. Gherghescu, A. V. Solov'yov, W. Greiner, Europhys. Lett. **88**, 23002 (2009).
14. D. N. Poenaru, R. A. Gherghescu, W. Greiner, Int.J. Mod. Phys. B **24**(17), 3411–3423 (2010).
15. D. N. Poenaru, R. A. Gherghescu, W. Greiner, J. Phys. G: Nucl. Part. Phys. **36**, 125101 (2009).
16. D. N. Poenaru, W. Greiner, Nucl. Phys. A **834**, 163c–166c (2010).
17. D. N. Poenaru, R. A. Gherghescu, W. Greiner, J. Phys. G: Nucl. Part. Phys. **37**(8), 085101 (2010).
18. D. N. Poenaru, W. Greiner, in *Clusters in Nuclei Vol. 1. Lecture Notes in Physics*, C. Beck, ed., vol. 818, chap. 1, pp. 1–56 (Springer, Berlin, 2010).
19. D. N. Poenaru, R. A. Gherghescu, I. H. Plonski, A. V. Solov'yov, W. Greiner, Rom. J. Phys. **54**(5-6), 457–466 (2009).
20. D. N. Poenaru, R. A. Gherghescu, I. H. Plonski, A. V. Solov'yov, W. Greiner, in *Latest Advances in Atomic Cluster Collisions*, Proc. of the International Symposium on Atomic Cluster Collisions: structure and dynamics from the nuclear to the biological scale, GSI Darmstadt, 2007, J.-P. Connerade, A. V. Solov'yov, eds., p. 128137 (Imperial College Press, London, 2008).
21. R. A. Gherghescu, D. N. Poenaru, A. V. Solov'yov, W. Greiner, Physica E **42**, 1555–1562 (2010).
22. R. A. Gherghescu, D. N. Poenaru, A. V. Solov'yov, W. Greiner, Europ. Phys. J. B **77**(1), 123–132 (2010).
23. D. N. Poenaru, I. H. Plonski, Rom. Rep. Phys. **60**(4), 529–538 (2008).
24. D. N. Poenaru, in *Exotic Nuclei and Nuclear/Particle Astrophysics (II)*, Proc. Carpathian Summer School of Physics, Sinaia, Romania, 2007, L. Trache, S. Stoica, eds., pp. 165–173 (AIP Conference Proceedings No. 972, Melville, NY, 2008).
25. D. N. Poenaru, R. A. Gherghescu, I. H. Plonski, A. V. Solov'yov, W. Greiner, J. Phys.: Conf. Ser. **111**, 012047 (2008).
26. D. N. Poenaru, R. A. Gherghescu, A. V. Solov'yov, W. Greiner, in *Proc. of The Fourth International Symposium on Atomic Cluster Collisions: structure and dynamics from the nuclear to the biological scale (ISACC09), Ann Arbor, MI, USA, July 14-18, 2009*, A. V. Solov'yov, E. Surdu-

tovich, eds., pp. 48–56 (AIP Conf. Proc. No. 1197, New York, 2009).
27. C. Bréchignac, P. Cahuzac, F. Carlier, J. Leygnier, A. Sarfati, Phys. Rev. B **44**, 11386–11393 (1991).
28. C. Bréchignac, P. Cahuzac, F. Carlier, M. de Frutos, Phys. Rev. B **49**, 2825–2831 (1994).
29. U. Näher, S. Frank, N. Malinowski, U. Zimmermann, T. P. Martin, Z. Phys. D **31**, 191–197 (1994).
30. S. Krückeberg, G. Dietrich, K. Lützenkirchen, L. Schweikhard, J. Ziegler, Phys. Rev. A **60**(2), 1251–1257 (1999).
31. H. J. Krappe, Z. Phys. D **23**, 269–274 (1992).
32. H. Koizumi, S. Sugano, Y. Ishii, Z. Phys. D **28**, 223–234 (1993).
33. U. Näher, S. Bjørnholm, S. Frauendorf, F. Garcias, C. Guet, Phys. Rep. **285**, 245–322 (1997).